MDA5 score–A Novel Lung Computed Tomography Scoring Method for Anti-Melanoma Differentiation-associated Gene 5-positive Dermatomyositis

Wenwen Xu
Shanghai Jiao Tong University School of Medicine Affiliated Renji Hospital https://orcid.org/0000-0003-2605-2127
Wanlong Wu
Shanghai Jiao Tong University School of Medicine Affiliated Renji Hospital
Danting Zhang
Shanghai Jiao Tong University School of Medicine Affiliated Renji Hospital
Zhiwei Chen
Shanghai Jiao Tong University School of Medicine Affiliated Renji Hospital
Yu Zheng
Shanghai Jiao Tong University School of Medicine Affiliated Renji Hospital
Xinwei Tao
Siemens Healthineers: Siemens Healthcare GmbH
Jiangfeng Zhao
Shanghai Jiao Tong University School of Medicine Affiliated Renji Hospital
Kaiwen Wang
Shanghai Jiao Tong University School of Medicine Affiliated Renji Hospital
Xiaodong Wang
Shanghai Jiao Tong University School of Medicine Affiliated Renji Hospital
Shuang Ye (ye_shuang2000@163.com)
Shanghai Jiao Tong University School of Medicine Affiliated Renji Hospital

Research article

Keywords: anti-melanoma differentiation-associated gene 5 antibody, dermatomyositis, interstitial lung disease, computed tomography scoring, artificial intelligence

Posted Date: February 22nd, 2021

DOI: https://doi.org/10.21203/rs.3.rs-198304/v1

Abstract

Background: Anti-melanoma differentiation-associated gene 5 (MDA5)-positive dermatomyositis (DM)-associated interstitial lung disease (ILD) is a life-threatening disease with a 6-month mortality as high as 50%. Evaluation of pulmonary high-resolution computed tomography (HRCT) is crucial in the prognostic prediction. This study aimed to develop a novel CT visual scoring method for anti-MDA5 positive DM-ILD.

Methods: A prospective cohort of hospitalized patients with anti-MDA5 positive DM-ILD was analyzed, and was further divided into a derivation dataset and a validation dataset. The primary outcome was the six-month all-cause mortality since the time of admission. Three components of baseline pulmonary CT images, i.e., ground glass opacity (GGO), consolidation and fibrosis were semi-quantitatively calculated in different lung lobes. The multivariable COX proportional hazards model was used to identify independent prognostic risk factors and corresponding coefficients, based upon which a scoring model was constructed. In addition, an artificial intelligence (AI) algorithm-based analysis and an idiopathic pulmonary fibrosis (IPF)-based scoring were conducted as comparators. The prediction accuracy of different methods was measured and compared by Harrell concordance index (C-index).

Results: Overall, 173 eligible patients were included. A novel GGO and consolidation-weighted CT visual scoring model for anti-MDA5 positive DM-ILD, namely 'MDA5 score', was developed with C-index values of 0.80 (95%CI 0.75-0.86) in the derivation dataset (n=116) and 0.84 (95%CI 0.71-0.97) in the validation dataset (n=57), respectively. While, the AI algorithm-based analysis, namely 'AI score', yielded C-index 0.78 (95%CI 0.72-0.84) for the derivation dataset and 0.77 (95%CI 0.64-0.90) for the validation dataset. 'MDA5 score' outperformed and IPF-based scoring ('IPF score') with respect to discrimination and clinical usefulness.

Conclusions: The novel derived 'MDA5 score' may serve as an applicable prognostic predictor for anti-MDA5 positive DM-ILD and facilitate further clinical trial design. The AI based CT quantitative analysis from COVID-19 provided a promising solution for ILD evaluation.

Background

Anti-melanoma differentiation-associated gene 5 (MDA5)-positive dermatomyositis (DM) is a special subtype of dermatomyositis (DM), associated with rapidly progressive interstitial lung disease (ILD). The overall prognosis is grave with 33-67% six-month mortality despite of aggressive immunosuppressive therapy (1-4).

Pulmonary high-resolution computed tomography (HRCT) is a main-stream imaging tool for identifying ILD and measuring its severity. A semi-quantitative HRCT scoring system has been applied as a prognostic prediction measurement in anti-MDA5 positive DM-ILD (5, 6). However, the applied scoring system was initially designed for evaluation of idiopathic pulmonary fibrosis (IPF) (7, 8). Therefore, when referring to a more rapid progressive disease, such as anti-MDA5 positive DM-ILD, the applicability has not been extensively validated. As examples, fibrosis components such as traction bronchiectasis (TBE) and honeycombing changes were higher weighted in this 'IPF score'; whereas inflammation components, i.e., ground-glass opacity (GGO) and consolidation were less weighted. Only until recently, another simplified scoring method for anti-MDA5 positive DM-ILD was proposed with equally weighted two components of GGO and fibrosis (9, 10). Unfortunately, the sample size was small with characteristic consolidation feature being overlooked; further independent evaluation in a data-driven approach is warranted. It is noteworthy that the time-consuming observer-dependent manner of these visual scorings is always an issue.

Under the pressure of the coronavirus disease 2019 (COVID-19) pandemic, advanced machine learning-based technologies on pulmonary CT quantitative analysis have rapidly emerged, providing a promising solution for diffuse lung disease HRCT evaluation in a more comprehensive and objective perspective (11-13).

Thus, the aims of the current study were to establish a novel pulmonary HRCT visual scoring method for predicting the six-month mortality in a large single-centered cohort of patients with anti-MDA5 positive DM; and in parallel, to explore

quantitative imaging assessment of this disease by applying artificial intelligence (AI) algorithm.

Materials And Methods

Patients

A prospective cohort of hospitalized patients with anti-MDA5 positive DM-ILD was setup since April 2014 in our center. All patients initially fulfilled Bohan and Peter's criteria for DM or Sontheimer's criteria for clinically amyopathic dermatomyositis on admission (14, 15), were re-evaluated retrospectively and considered eligible as long as they also met the recent 239th ENMC classification criteria for DM (16). All patients were with imaging-confirmed ILD and positive anti-MDA5 antibody. The anti-MDA5 antibody was detected by immunoblotting assay (Euroimmun, Germany) and confirmed by ELISA (Supplementary Data S1). ILD course was defined as time from the first abnormal pulmonary CT which revealed ILD changes to admission. Patients with ILD course > 3 months or with coexisting malignancy (within 3 years) or with pre-existing chronic obstructive pulmonary disease were excluded. The primary outcome was the six-month all-cause mortality since the time of admission.

A total of 173 eligible patients were enrolled and were further divided into two datasets. Patients admitted between April 2014 and December 2018 (n=116) versus those admitted between January 2019 and January 2020 (n=57), were defined as the derivation dataset and the validation dataset, respectively (Figure 1).

Clinical data including age, gender, physical findings, respiratory function, treatment history and outcomes were obtained from medical records. The study protocol was approved by the ethics committees of our hospital and the need to obtain informed consent was waived.

HRCT images acquisition and visual scoring

Patients underwent non-contrast pulmonary HRCT at the day around admission (median, 2 days; range, 1–6 days), using multidetector CT scanner (United Imaging, Shanghai, China; Siemens Healthineers, Forchheim, Germany). CT slice thickness was 1.0–1.5mm at 10mm intervals in the whole lungs.

All CT images were reviewed by two observers (YZ with 10-years' experience and CZ with 5-years' experience in chest HRCT imaging evaluation) who were blinded to patients' outcome. Inter-observer variability was evaluated by Intraclass correlation coefficient (ICC). The results were agreed upon by consensus between the two observers.

For the previously reported IPF-based visual scoring method ('IPF score'), HRCT findings were evaluated for GGO, consolidation, TBE and honeycombing defined by the Fleischner Society, and were graded on a scale of 1-6 based on the classification system (8). The overall 'IPF score' was calculated by summing the average score of six zones (upper, middle, and lower on both sides) as described; and was used as a comparator for the following analysis.

Three components, i.e. GGO, consolidation and fibrosis, were separately rated and recorded according to pulmonary involvement area of the five lobes (right upper, right middle, right lower, left upper and left lower lobes of the lung). The 0–5 scoring for GGO or consolidation at each lobe was adopted (0, no involvement; 1, ≤5% involvement; 2, 5 to <25% involvement; 3, 25-49% involvement; 4, 50-75% involvement; 5, >75% involvement). Similarly, the fibrotic change in each lobe was classified into 5 grades (0, no fibrosis; 1, interlobular septal thickening without honeycombing; 2, honeycombing < 25%; 3, 25-49%; 4, 50-75%; 5, > 75% of the lobe) as fibrosis score (9, 10). The respective total score of each component (GGO, consolidation and fibrosis) was the sum of each lobe's score and ranged from 0 (no involvement) to 25 (maximum involvement).

AI algorithm-based CT quantitative analysis

The Digital Imaging and Communications in Medicine files of CT images were inputted and run on a software package named “CT Pneumonia Analysis” (syngo.via Frontier 1.0, Siemens Healthineers, Forchheim, Germany). The algorithm had been first trained on a large cohort of patients with various diseases, then fine-tuned with a cohort with abnormal patterns including GGO, consolidation, effusions, and masses, to improve the robustness of the lung segmentation over the involved areas. Based on 3D segmentations of lesions, lungs, and lobes, the AI algorithm automatically detected and quantified abnormal tomographic patterns commonly present in pneumonia, such as GGO and consolidation both globally and lobe-wise.

The percentage of total opacity (total lesions) as well as the percentage of consolidation (with a cutoff of CT value≥-200 Hounsfield unit) was directly calculated for the whole lung. Then by subtracting consolidation from total lesion, the percentage of GGO was obtained for further analysis.

Statistical Analysis

Clinical data were described and compared between the derivation and validation datasets by univariable analysis. The Mann-Whitney U test, Chi-square test and Fisher's exact test were conducted, as appropriate. Clinical features with >5% missing data were excluded for analysis.

Among the three visual scoring components, i.e. GGO, consolidation and fibrosis, variables significantly associated with outcome in the univariable analysis were subsequently included in the multivariable COX proportional hazards model. The derived β regression coefficients were used to construct a linear weighted scoring model, defined as ‘MDA5 score’. Likewise, the percentage of GGO and consolidation from AI algorithm based quantitative analysis were used to construct another weighted scoring model, defined as ‘AI score’.

The optimal cutoff value of CT score was identified by receiver operating characteristic curve analysis. The association between CT score and six-month survival were assessed by Kaplan-Meier survival plot and log-rank test.

Model discrimination of the ‘IPF score’, ‘MDA5 score’ and ‘AI score’ models were quantified and compared by the Harrell concordance index (C-index) with 95% confidence interval (CI). A decision curve analysis (DCA) was built to determine and compare the clinical usefulness of each model(17). Significance was defined as $p<0.05$.

Statistical analyses were performed by SPSS software version 25 (IBM Corp., Armonk, NY, USA), and R software version 3.6.1 (http://www.Rproject.org). All the R codes were available at Github (https://github.com/tomato08217/MDA5).

Results

Comparable baseline clinical features, treatment and outcomes of the derivation dataset and validation dataset were listed in Supplementary table S1. Of which, 47 (40.5%) and 21 (36.8%) patients died within six-month follow up since the time of admission, respectively (p=0.764).

‘MDA5 score’: a novel CT visual Semi-Quantitative Analysis

The pulmonary HRCT findings from visual semi-quantitative analysis of patients between survivors and non-survivors in both datasets were presented in Table 1. As expected, the ILD pattern distributed bilaterally. It was noteworthy that only GGO and consolidation patterns were significantly associated with outcome according to univariable analysis; as opposed to neither fibrosis nor the presence of pneumomediastinum or pneumothorax (PNM) at baseline. Then, the GGO and consolidation score were included in further multivariable COX regression analysis. Both total GGO score (β coefficient=0.13, $p<0.001$) and total consolidation score (β coefficient=0.22, $p<0.001$) were determined to be significantly associated with all-cause mortality

(Table 2). To simplify, a linear equation, namely 'MDA5 score', by combining defined prognostic factors weighted by their β coefficients was finally generated: total GGO score+2*total consolidation score.

ROC curve analysis indicated that the optimal cutoff value for 'MDA5 score' was 18, which could efficiently predict the six-month all-cause mortality in the derivation dataset (sensitivity 70.2%; specificity 82.6%) and the validation dataset (sensitivity 85.7%; specificity 63.9%). The prediction accuracy of 'MDA5 score' calculated by AUC was 0.85 (95%CI 0.78-0.91) for the derivation dataset and 0.87 (95%CI 0.78-0.96) for the validation dataset, far ahead of the 'IPF score', which was 0.81 (95%CI 0.73-0.89) for the derivation dataset and 0.79 (95%CI 0.68-0.91) for the validation dataset. Additionally, The Kaplan-Meier survival plots of patients in both datasets presented significant difference between the high-risk ('MDA5 score'>18) and low-risk ('MDA5 score'≤18) groups (Figure 2). The mortality of high-risk patients was 73.3% in the derivation dataset and 58.1% in the validation dataset; while the mortality of low-risk patients was 19.7% in the derivation dataset and 11.5% in the validation dataset.

'AI score': an AI algorithm-based Quantitative Analysis

The redundancy of the baseline fibrosis component in terms of outcome prediction made pneumonia-trained AI algorithm plausible for our anti-MDA5 positive DM-ILD patients' CT quantitative analysis (Figure 3A). Percentage of consolidation was determined as the only significant predictor for the overall survival in the final multivariable COX model ($p<0.001$) (Table 2). Thus, the percentage of consolidation was defined to represent 'AI score'. Interestingly, the radar charts in Figure 3B showed that the GGO and consolidation patterns were symmetrically distributed, with an evident 'gravity gradient' propensity to the lower area of the lungs, especially for the consolidation distribution.

Comparisons of Clinical Performance between 'IPF score', 'MDA5 score' and 'AI score' model

The inter-observer consistency of the two visual scoring models was assessed with an ICC of 0.69 (95% CI 0.57–0.78) for 'IPF score' and an ICC of 0.93 (95% CI 0.89-0.96) for 'MDA5 score'. Therefore, 'MDA5 score' attained a better inter-observer reproducibility. Hereafter, the comparisons of model discrimination between 'IPF score', 'MDA5 score' and 'AI score' were shown in Table 3. Notably, 'MDA5 score' had the best performance with C-index values of 0.80 (95%CI 0.75-0.86) in the derivation dataset and 0.84 (95%CI 0.71-0.97) in the validation dataset, respectively. While, 'AI score' yielded C-index 0.78 (95%CI 0.72-0.84) for the derivation dataset and 0.77 (95%CI 0.64-0.90) for the validation dataset. Finally, the DCA further demonstrated that the 'MDA5 score' also presented with a higher overall net benefit than the other two models in terms of clinical applicability (Figure 4).

Discussion

As a highly progressive disease, anti-MDA5 positive DM-ILD remains to be a big challenge despite of recent treatment advances (4, 18). Several prognostic indicators of the disease had been reported involving respiratory physiology parameters, laboratory biomarkers, and radiology features (1, 6, 19). The current study focused on patients' baseline pulmonary HRCT and attempted to quantitatively assess the disease in the regard of predicting six-month mortality.

Our study takes a step-forward from the previous visual scoring methods, and extensively evaluates the distribution and extent of three basic imaging components of anti-MDA5 positive DM-ILD, i.e., GGO, consolidation and fibrosis. In line with prior reports, our data confirmed that the presence of fibrosis or TBE in the context of GGO or consolidation, is not of predictive value on prognosis in anti-MDA5 positive DM-ILD (5, 10). The probable explanation is that those fibrotic features are less common in this rapid progressive disease and likely to be presented, if it happens, in later stage instead of baseline. The same notion apparently holds true for the presence of PNM, which is a known severity indicator rather than a baseline predictor (20).

The combination of the extent of GGO and consolidation was found to have the best yield in terms of outcome prediction, with the area of consolidation contributing more than GGO. The image ‘snapshot’ might reflect the dynamic transformation from GGO to consolidation as disease progresses, just like the imaging changes observed in severe COVID-19 patients (11, 12, 21). A possible shared underlying mechanism of acute lung injury in the two diseases is a very intriguing question deserves further investigation. After all, the highly activated type I interferon pathway in anti-MDA5 positive DM-ILD which suggested a possible virus-triggered response has been postulated(22, 23).

To apply AI algorithm-based quantitative imaging analysis in anti-MDA5 positive DM-ILD is a preliminary yet novel attempt. The primary targets of the algorithm were for those pneumonia patients, or more specifically, COVID-19 patients. Of interest, our data suggested that this AI algorithm performs fairly well among anti-MDA5 positive DM-ILD patients. The performance might be further enhanced given more anti-MDA5 positive DM-ILD imaging data could be fed into its machine-learning processes.

The major limitation of our study was the single-center design. Although we presented a relatively large cohort for this rare disease and performed internal validation, large-scale multi-center external validation is mandatory before the CT scoring models being utilized in a clinical setting. Based upon this, the biases of different machine conditions, patient selection and treatment protocols could be taken into consideration and subjected to better control and adjustment. In addition, longitudinal analysis on the changes of ILD patterns over time remains untouched in the current study, which deserves further exploration.

Conclusions

We have shown that a GGO and consolidation-weighted CT scoring model, along with an AI algorithm, might serve as prognostic predictors for six-month mortality in anti-MDA5 positive DM-ILD. This might facilitate future clinical trial design and precision management for this tricky disease.

List Of Abbreviations

AI: Artificial intelligence

C-index: The Harrell concordance index

CI: Confidence interval

COVID-19: The coronavirus disease 2019

DCA: Decision curve analysis

DM: Dermatomyositis

GGO: Ground-glass opacity

HRCT: High-resolution computed tomography

ICC: Intraclass correlation coefficient

ILD: Interstitial lung disease

IPF: Idiopathic pulmonary fibrosis

MDA5: Melanoma differentiation-associated gene 5

PNM: Pneumomediastinum or pneumothorax

TBE: Traction bronchiectasis

Declarations

Ethics approval and consent to participate

The study was approved by the Shanghai Jiaotong University School of Medicine, Renji Hospital Ethnics Committee. The need to obtain informed consent was waived.

Consent for publication

We obtained consent for publication from all the individuals whose detailed information was included in this manuscript.

Availability of data and materials

The datasets used and/or analyzed during the current study are available from the corresponding author upon reasonable request.

Competing Interests

SY has received speaker's and consulting fees from Abbvie, Jansen Biologics, GlaxoSmithKline, Roche, and Pfizer, and grants from Pfizer. All the other authors have nothing to disclose.

Funding

No specific funding was received from any bodies in the public, commercial or not-for-profit sectors to carry out the work described in this article.

Authors' contributions

WX, WW, XW, SY contributed to the project design. WX, WW, ZC, DZ collected the clinical data of patients. JZ, KW were responsible for laboratory data. YZ contributed to the assessment of pulmonary function tests. ZC, YZ carried out visual HRCT evaluation. WX, XT operated the CT pneumonia analysis software. WX, WW, DZ, XT contributed to analysis of all data. WX, WW, SY wrote and revised the manuscript. All authors read and approved the final manuscript.

Acknowledgement

Not applicable.

References

1. Gono T, Sato S, Kawaguchi Y, Kuwana M, Hanaoka M, Katsumata Y, et al. Anti-MDA5 antibody, ferritin and IL-18 are useful for the evaluation of response to treatment in interstitial lung disease with anti-MDA5 antibody-positive dermatomyositis.

Rheumatology (Oxford). 2012;51(9):1563-70.
2. Koga T, Fujikawa K, Horai Y, Okada A, Kawashiri SY, Iwamoto N, et al. The diagnostic utility of anti-melanoma differentiation-associated gene 5 antibody testing for predicting the prognosis of Japanese patients with DM. Rheumatology (Oxford). 2012;51(7):1278-84.
3. Ye S, Chen XX, Lu XY, Wu MF, Deng Y, Huang WQ, et al. Adult clinically amyopathic dermatomyositis with rapid progressive interstitial lung disease: a retrospective cohort study. Clin Rheumatol. 2007;26(10):1647-54.
4. Tsuji H, Nakashima R, Hosono Y, Imura Y, Yagita M, Yoshifuji H, et al. Multicenter Prospective Study of the Efficacy and Safety of Combined Immunosuppressive Therapy With High-Dose Glucocorticoid, Tacrolimus, and Cyclophosphamide in Interstitial Lung Diseases Accompanied by Anti-Melanoma Differentiation-Associated Gene 5-Positive Dermatomyositis. Arthritis Rheumatol. 2019.
5. Zou J, Guo Q, Chi J, Wu H, Bao C. HRCT score and serum ferritin level are factors associated to the 1-year mortality of acute interstitial lung disease in clinically amyopathic dermatomyositis patients. Clin Rheumatol. 2015;34(4):707-14.
6. Lian X, Zou J, Guo Q, Chen S, Lu L, Wang R, et al. Mortality risk prediction in amyopathic dermatomyositis associated with interstitial lung disease: the FLAIR model. Chest. 2020.
7. Kazerooni EA, Martinez FJ, Flint A, Jamadar DA, Gross BH, Spizarny DL, et al. Thin-section CT obtained at 10-mm increments versus limited three-level thin-section CT for idiopathic pulmonary fibrosis: correlation with pathologic scoring. AJR Am J Roentgenol. 1997;169(4):977-83.
8. Ichikado K, Suga M, Muranaka H, Gushima Y, Miyakawa H, Tsubamoto M, et al. Prediction of prognosis for acute respiratory distress syndrome with thin-section CT: validation in 44 cases. Radiology. 2006;238(1):321-9.
9. Fujiki Y, Kotani T, Isoda K, Ishida T, Shoda T, Yoshida S, et al. Evaluation of clinical prognostic factors for interstitial pneumonia in anti-MDA5 antibody-positive dermatomyositis patients. Mod Rheumatol. 2018;28(1):133-40.
10. Yamaguchi K, Yamaguchi A, Itai M, Kashiwagi C, Takehara K, Aoki S, et al. Clinical features of patients with anti-melanoma differentiation-associated gene-5 antibody-positive dermatomyositis complicated by spontaneous pneumomediastinum. Clin Rheumatol. 2019;38(12):3443-50.
11. Sun D, Li X, Guo D, Wu L, Chen T, Fang Z, et al. CT Quantitative Analysis and Its Relationship with Clinical Features for Assessing the Severity of Patients with COVID-19. Korean J Radiol. 2020;21(7):859-68.
12. Wang Y, Chen Y, Wei Y, Li M, Zhang Y, Zhang N, et al. Quantitative analysis of chest CT imaging findings with the risk of ARDS in COVID-19 patients: a preliminary study. Ann Transl Med. 2020;8(9):594.
13. Lanza E, Muglia R, Bolengo I, Santonocito OG, Lisi C, Angelotti G, et al. Quantitative chest CT analysis in COVID-19 to predict the need for oxygenation support and intubation. Eur Radiol. 2020.
14. Bohan A, Peter JB. Polymyositis and dermatomyositis (first of two parts). N Engl J Med. 1975;292(7):344-7.
15. Sontheimer RD. Would a new name hasten the acceptance of amyopathic dermatomyositis (dermatomyositis sine myositis) as a distinctive subset within the idiopathic inflammatory dermatomyopathies spectrum of clinical illness? J Am Acad Dermatol. 2002;46(4):626-36.
16. Mammen AL, Allenbach Y, Stenzel W, Benveniste O, Group EtWS. 239th ENMC International Workshop: Classification of dermatomyositis, Amsterdam, the Netherlands, 14-16 December 2018. Neuromuscul Disord. 2020;30(1):70-92.
17. KF K, MD B, K Z, Oncology JHJJocoojotASoC. Assessing the Clinical Impact of Risk Prediction Models With Decision Curves: Guidance for Correct Interpretation and Appropriate Use. 2016;34(21):2534-40.
18. Chen Z, Wang X, Ye S. Tofacitinib in Amyopathic Dermatomyositis-Associated Interstitial Lung Disease. N Engl J Med. 2019;381(3):291-3.
19. Wang K, Zhao J, Chen Z, Li T, Tan X, Zheng Y, et al. CD4+CXCR4+ T cells as a novel prognostic biomarker in patients with idiopathic inflammatory myopathy-associated interstitial lung disease. Rheumatology (Oxford). 2019;58(3):511-21.
20. Zhou M, Ye Y, Yan N, Lian X, Bao C, Guo Q. Noninvasive positive pressure ventilator deteriorates the outcome of pneumomediastinum in anti-MDA5 antibody-positive clinically amyopathic dermatomyositis. Clin Rheumatol. 2020.

21. Ruch Y, Kaeuffer C, Ohana M, Labani A, Fabacher T, Bilbault P, et al. CT lung lesions as predictors of early death or ICU admission in COVID-19 patients. Clin Microbiol Infect. 2020.
22. Sato S, Hoshino K, Satoh T, Fujita T, Kawakami Y, Fujita T, et al. RNA helicase encoded by melanoma differentiation-associated gene 5 is a major autoantigen in patients with clinically amyopathic dermatomyositis: Association with rapidly progressive interstitial lung disease. 2009;60(7):2193-200.
23. Nakashima R, Imura Y, Kobayashi S, Yukawa N, Yoshifuji H, Nojima T, et al. The RIG-I-like receptor IFIH1/MDA5 is a dermatomyositis-specific autoantigen identified by the anti-CADM-140 antibody. 2010;49(3):433-40.

Tables

Table 1: Comparison of visual CT features between two datasets with different outcome.

	Derivation dataset				Validation dataset				p-value†
	All (n=116)	Survivors (n=69)	Non-survivors (n=47)	p-value*	All (n=57)	Survivors (n=36)	Non-survivors (n=21)	p-value*	
Distribution pattern									
Bilateral lung involved	113 (97.4)	66 (95.7)	47 (100.0)	0.39	54 (94.7)	33 (91.7)	21 (100.0)	0.46	0.64
RU lobe involved	95 (81.9)	50 (72.5)	45 (95.7)	**0.003**	48 (84.2)	27 (75.0)	21 (100.0)	**0.03**	0.87
RM lobe involved	76 (65.5)	36 (52.2)	40 (85.1)	**0.001**	42 (73.7)	22 (61.1)	20 (95.2)	**0.01**	0.36
RL lobe involved	113 (97.4)	66 (95.7)	47 (100.0)	0.39	57 (100.0)	36 (100.0)	21 (100.0)	1	0.55
LU lobe involved	99 (85.3)	54 (78.3)	45 (95.7)	**0.02**	51 (89.5)	30 (83.3)	21 (100.0)	0.13	0.61
LL lobe involved	113 (97.4)	67 (97.1)	46 (97.9)	1	54 (94.7)	33 (91.7)	21 (100.0)	0.46	0.64
No. involved lobe				**0.001**				**0.02**	0.17
1	2 (1.7)	2 (2.9)	0 (0.0)		3 (5.3)	3 (8.3)	0 (0.0)		
2	12 (10.3)	11 (15.9)	1 (2.1)		1 (1.8)	1 (2.8)	0 (0.0)		
3	7 (6.0)	5 (7.2)	2 (4.3)		4 (7.0)	4 (11.1)	0 (0.0)		
4	26 (22.4)	21 (30.4)	5 (10.6)		10 (17.5)	9 (25.0)	1 (4.8)		
5	69 (59.5)	30 (43.5)	39 (83.0)		39 (68.4)	19 (52.8)	20 (95.2)		
No. involved lobes>3	95 (81.9)	51 (73.9)	44 (93.6)	**0.01**	49 (86.0)	28 (77.8)	21 (100.0)	0.05	0.65
No. involved lobes>4	69 (59.5)	30 (43.5)	39 (83.0)	**<0.001**	39 (68.4)	19 (52.8)	20 (95.2)	**0.002**	0.33
PNM	5 (4.3)	2 (2.9)	3 (6.4)	0.39	3	1 (2.8)	2 (9.5)	0.55	0.72
Scoring of three components									
Total GGO score	4 [2-8]	3 [2-6]	7 [3-10]	**<0.001**	6 [2-11]	5 [1-8]	10 [7-12]	**0.002**	0.13
Total CON score	4 [2-8]	3 [1-5]	8 [5-11]	**<0.001**	6 [4-9]	5 [2-7]	9 [7-13]	**<0.001**	0.06
Total fibrosis score	3 [2-5]	2 [2-4]	3 [2-5]	0.51	4 [2-5]	4 [2-5]	5 [2-5]	0.51	0.01

IPF score	126 [116-151]	118 [112-127]	147 [125-171]	**<0.001**	135 [121-155]	127 [112-141]	153 [134-188]	**<0.001**	0.12

Data are presented as median [IQR] for continuous variables and number (frequency) (%) for categorical variables.

***** A comparison between the survivors and non-survivors groups.

† A comparison between the derivation and validation datasets.

CT, computed tomography; RU, right upper; RM, right middle; RL, right lower; LU, left upper; LL, left lower; PNM, pneumomediastinum or pneumothorax; GGO, ground-glass opacity; CON, consolidation; IPF score, idiopathic pulmonary fibrosis based visual scoring method.

Table 2: Multivariable COX regression analysis for 'MDA5 score' and 'AI score' models.

	HR [95%CI]	P-value	β coefficient
'MDA5 score' model			
total GGO score	1.14 [1.06-1.22]	<0.001	0.13
total consolidation score	1.25 [1.16-1.34]	<0.001	0.22
'AI score' model			
percentage of GGO	1.02 [1.00, 1.04]	0.07	0.02
percentage of consolidation	1.15 [1.08, 1.22]	<0.001	0.14

HR, hazard ratio; 95%CI, 95% confidence interval; MDA5, anti-melanoma differentiation-associated gene 5; AI, artificial intelligence; GGO, ground-glass opacity.

Table 3: Comparison of the prediction performance of each model.

Scoring model	C-index [95%CI]	
	derivation dataset (n=116)	validation dataset (n=57)
'IPF score'	0.78 [0.71-0.84]	0.78 [0.65-0.91]
'MDA5 score' *	0.80 [0.75-0.86]	0.84 [0.71-0.97]
total GGO score+2*total consolidation score		
'AI score'	0.78 [0.72-0.84]	0.77 [0.64-0.90]
percentage of consolidation		

***** 'MDA5 score' model performed significantly better than 'IPF score' model (p=0.02).

C-index, concordance index; 95%CI, 95% confidence interval; IPF, idiopathic pulmonary fibrosis; MDA5, anti-melanoma differentiation-associated gene 5; GGO, ground-glass opacity; AI, artificial intelligence.

Figures

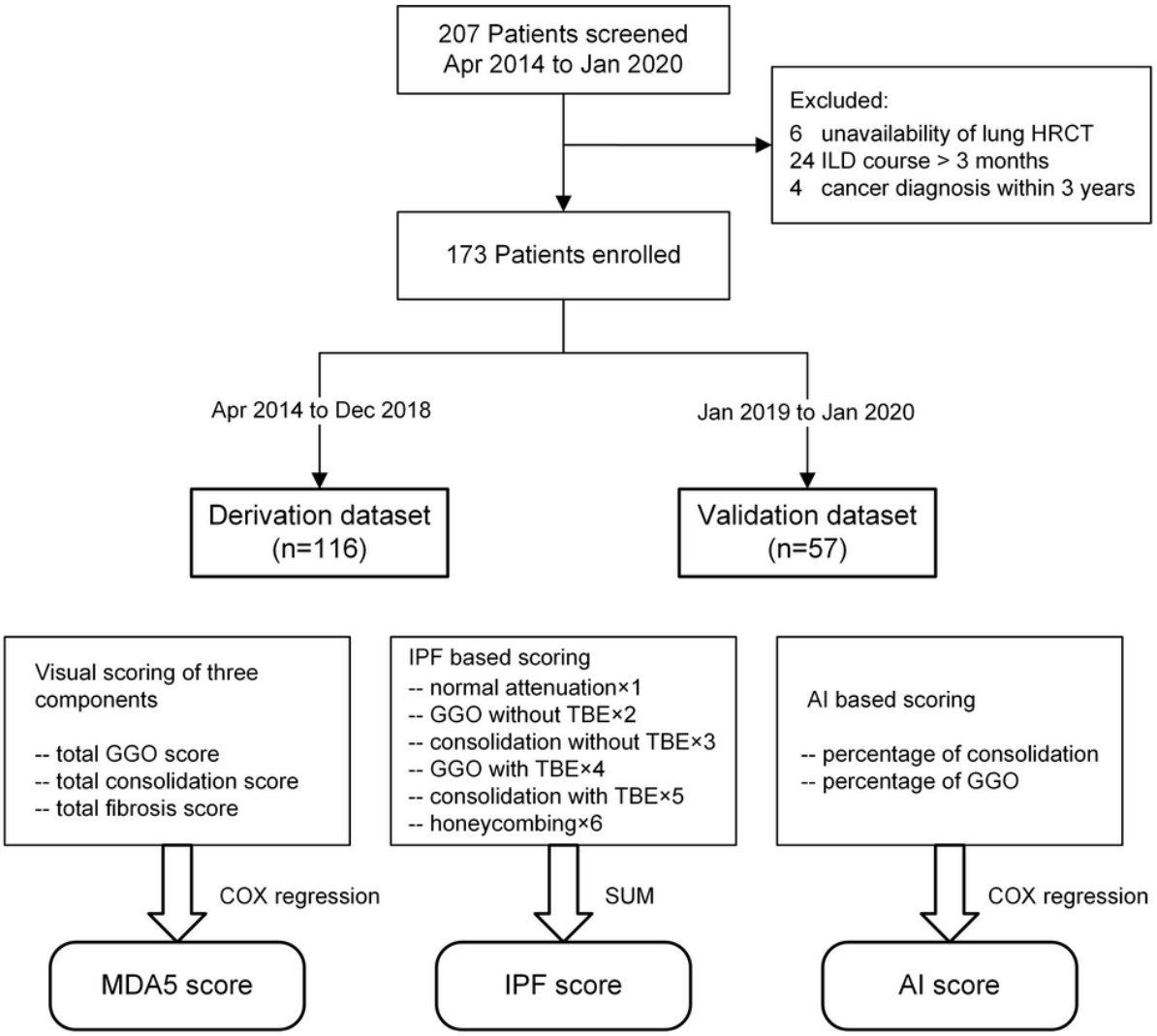

Figure 1

Flow chart of patients and three CT scoring models. MDA5, melanoma differentiation-associated gene 5; HRCT, high-resolution computed tomography; ILD, interstitial lung disease; GGO, ground-glass opacity; TBE, traction bronchiectasis; IPF, idiopathic pulmonary fibrosis; AI, artificial intelligence; DM, dermatomyositis.

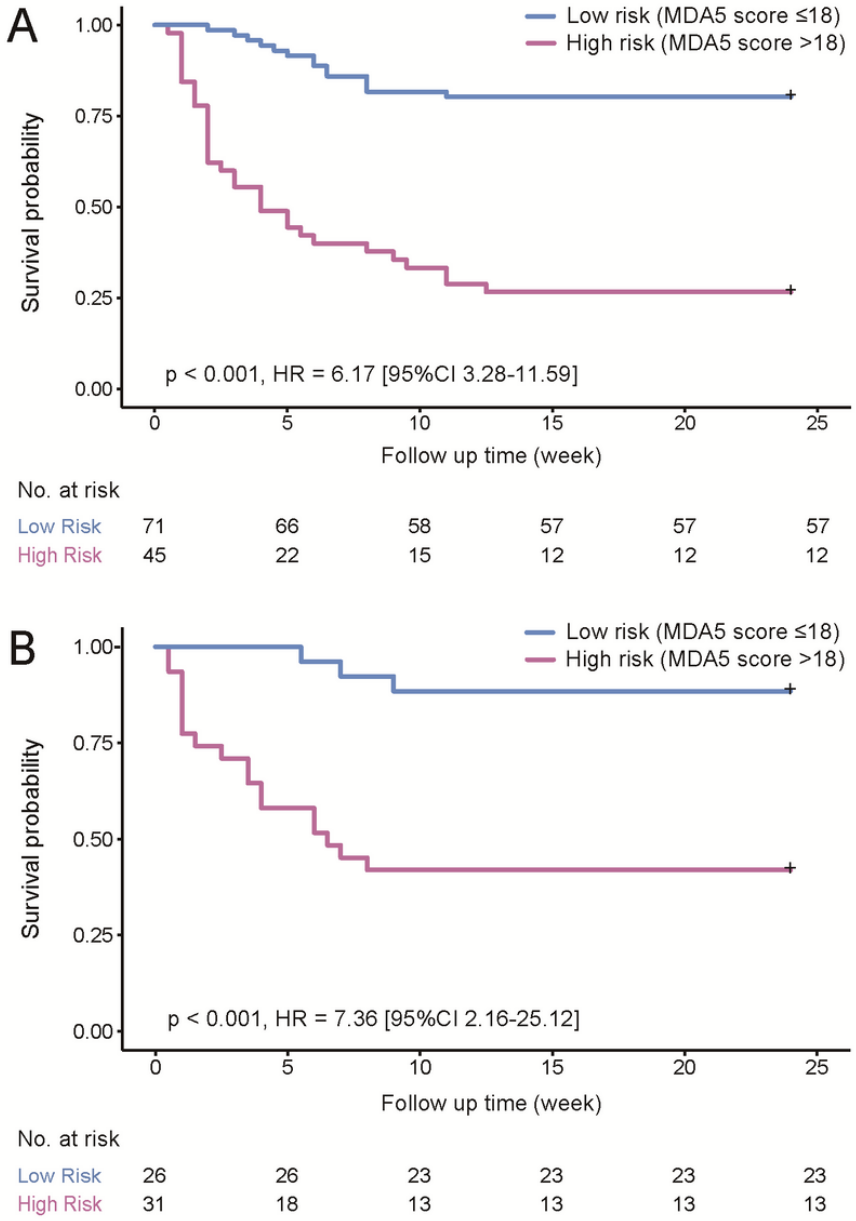

Figure 2

Survival curves of 'MDA5 score' in the derivation (A) and validation (B) datasets. MDA5, melanoma differentiation-associated gene 5; HR, hazard ratio; 95%CI, 95% confidence interval.

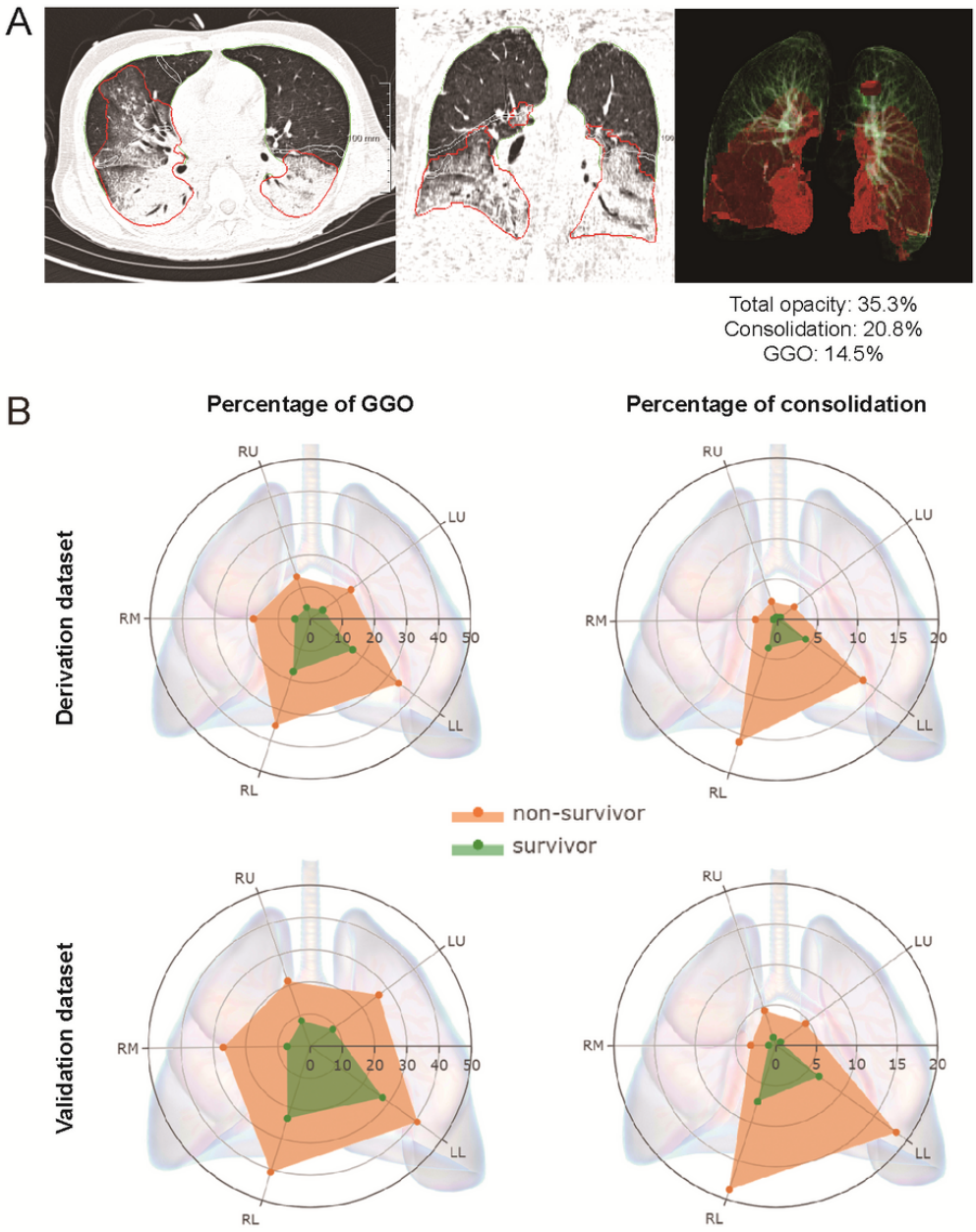

Figure 3

Artificial intelligence algorithm-based CT quantitative analysis. (A) The segmentation results of the lung and its total opacity in representative CT images were shown in green and red borders respectively. The percentage of total opacity, consolidation, and ground-glass opacity (GGO) of the whole lung were automatically calculated to be 35.3%, 20.8%, and 14.5% respectively. (B) The average distributions of GGO and consolidation in each lobe of the lung were displayed by the radar charts in both datasets. The axial line of the radar chart referred to the mean percentage (%) of either GGO or consolidation of each lobe. RU, right upper lobe; RM, right middle lobe; RL, right lower lobe; LU, left upper lobe; LL, left lower lobe.

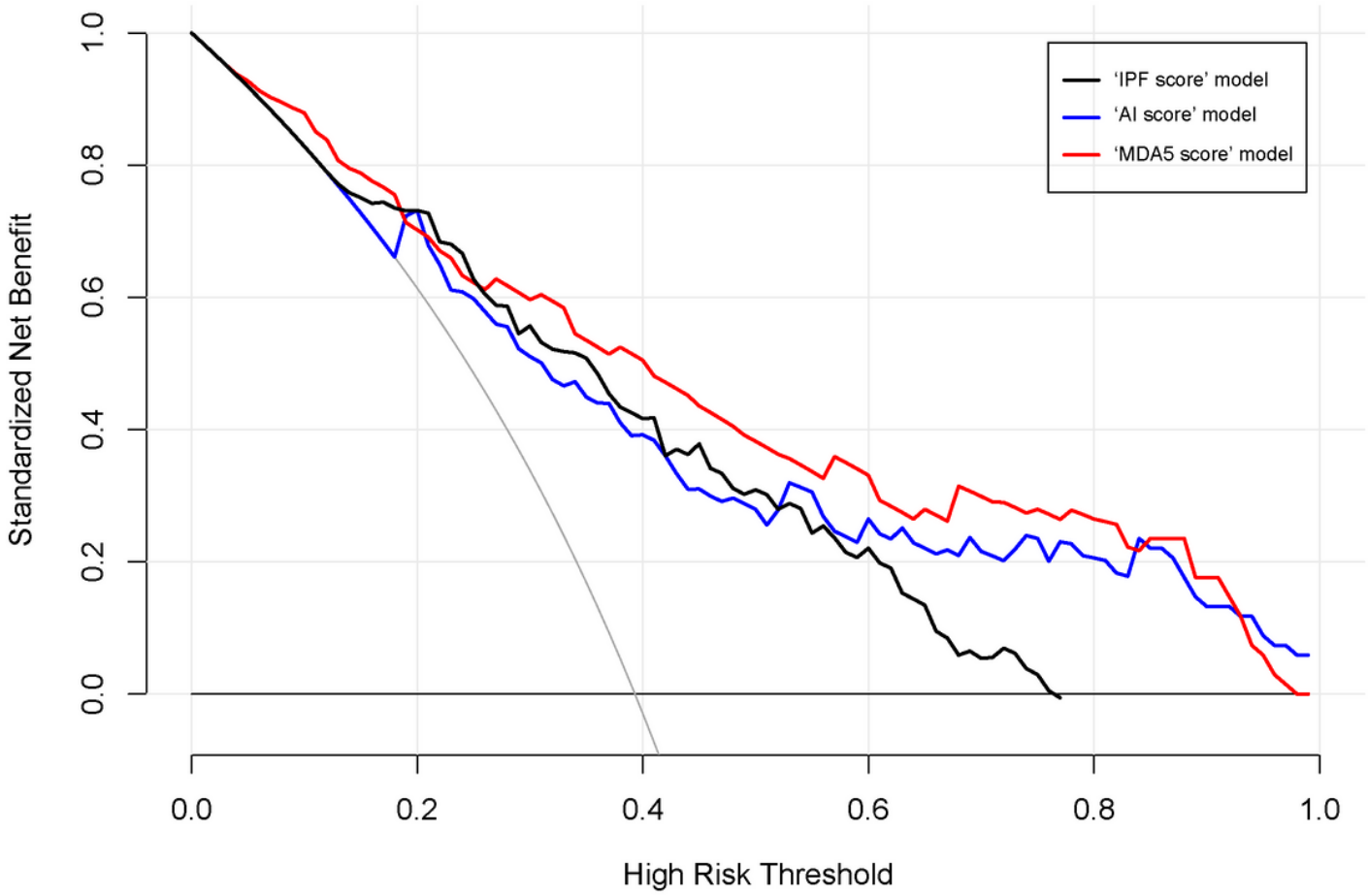

Figure 4

Decision curve analysis for 'IPF score', 'MDA5 score' and 'AI score' model. The concept of population net benefit (NB) is fundamental to decision curves (measured in the y-axis) and referred to classification accuracy of a model. Suppose high risk is defined as risk above some risk threshold R (x-axis); such high-risk patients are recommended an intervention. The NB of using the risk model was calculated by the true-positive rate, the proportion of cases with risk above risk threshold R; and the false-positive rate, the proportion of controls with risk above risk threshold R. The horizontal dotted line at NB = 0 mean a simple policy of no intervention to all patients (treat none); the gray curve in the plot depicted the NB of another simple policy: recommend the intervention to everyone regardless of risk. In our result, the 'MDA5 score' model (red line) had the highest net benefit compared to the others, almost across the full range of threshold probabilities.

Supplementary Files

This is a list of supplementary files associated with this preprint. Click to download.

- SupplementaryDataS1.docx
- SupplementarytableS1.docx